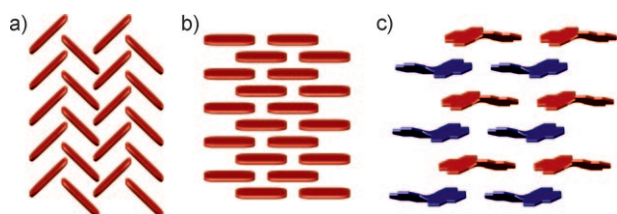


# A Crystal-Engineered Hydrogen-Bonded Octachloroperylene Diimide with a Twisted Core: An n-Channel Organic Semiconductor\*\*

Marcel Gsänger, Joon Hak Oh, Martin Könemann, Hans Wolfgang Höffken, Ana-Maria Krause, Zhenan Bao,\* and Frank Würthner\*

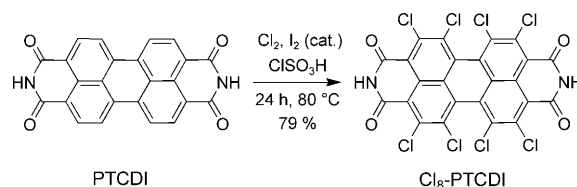
The appropriate arrangement of organic semiconductors in the solid state is decisive for efficient charge-carrier transport between source and drain electrodes in organic thin-film transistors (OTFTs).<sup>[1]</sup> However, the still unsolved challenges in crystal engineering<sup>[2]</sup> mean that there are only few examples where the packing of  $\pi$ -conjugated semiconductors can be controlled by means of rational design concepts to avoid the most common herringbone  $\pi$ -stacking motif (Figure 1a).<sup>[3]</sup> An outstanding example is provided by the



**Figure 1.** Crystal engineering concepts to replace the common one-dimensional herringbone  $\pi$ -stacking motif (a) by planar (b) or contorted (c) brickstone arrangements that provide two-dimensional percolation paths for charge-carrier transport in organic semiconductors. In (c), the *M* enantiomers are shown in red and *P* enantiomers in blue.

silylethynylacenes reported by Anthony and co-workers. In this example, bulky triisopropylsilyl substituents direct a slipped brickstone arrangement of pentacene and dithienoanthracene molecules that afford excellent p-channel field-effect mobilities of around  $1\text{ cm}^2\text{V}^{-1}\text{s}^{-1}$  (Figure 1b).<sup>[3a,b]</sup> Likewise, dichloro substitution on the periphery of the tetracene core resulted in face-to-face packing and a single-crystal field-effect mobility of  $1.6\text{ cm}^2\text{V}^{-1}\text{s}^{-1}$  was reported, whereas a mobility of  $10^{-4}\text{ cm}^2\text{V}^{-1}\text{s}^{-1}$  was reported for the herringbone-

packed monochloro derivative.<sup>[3c]</sup> These high values are attributed to close  $\pi$ - $\pi$  contacts between acenes in two crystallographic directions. According to another concept introduced by one of our research groups, a slipped two-dimensional  $\pi$ -stacked arrangement should be possible upon twisting of the  $\pi$ -conjugated organic semiconductor core (Figure 1c).<sup>[4]</sup> However, only moderate field-effect mobilities of  $0.02\text{ cm}^2\text{V}^{-1}\text{s}^{-1}$  for contorted hexabenzocoronenes<sup>[5]</sup> and  $0.11\text{ cm}^2\text{V}^{-1}\text{s}^{-1}$  for 1,6,7,12-tetrachloro-substituted perylene-3,4:9,10-tetracarboxylic diimides ( $\text{Cl}_4$ -PTCDI)<sup>[6]</sup> could be achieved for compounds designed according to this concept. After analysis of the packing deficiencies of our earlier PTCDI derivatives,<sup>[4,6]</sup> we have now synthesized a new derivative  $\text{Cl}_8$ -PTCDI (see Scheme 1) that bears eight chlor-



**Scheme 1.** Synthesis of  $\text{Cl}_8$ -PTCDI.

ine substituents at the aromatic core and free NH imide functionalities. By increasing the number of chlorine substituents from four to eight, a “brick” with sides of similar dimensions is formed, in which the free NH imide groups were envisioned to enforce a close hydrogen-bonded contact between adjacent molecules.<sup>[7]</sup> Herein, we show that the molecular organization can indeed be governed by the crystal engineering concept outlined in Figure 1c, and that n-channel field-effect transistors with excellent mobilities of almost  $1\text{ cm}^2\text{V}^{-1}\text{s}^{-1}$  and on-to-off current ratios greater than  $10^6$  are obtained for thin films of our new compound  $\text{Cl}_8$ -PTCDI.<sup>[8]</sup>

1,2,5,6,7,8,11,12 - Octachloroperylene - 3,4:9,10 - tetracarboxylic diimide ( $\text{Cl}_8$ -PTCDI) was obtained as an orange solid by chlorination of perylene-3,4:9,10-tetracarboxylic diimide in chlorosulfonic acid at  $80^\circ\text{C}$  in 79% yield (Scheme 1, for details see the Supporting Information).<sup>[9]</sup>

To ensure the high purity needed for incorporation into devices,  $\text{Cl}_8$ -PTCDI was purified by successive recrystallizations from *N*-methylpyrrolidone (NMP) and acetic acid, and finally by gradient sublimation (temperature range  $250$ – $400^\circ\text{C}$  at  $10^{-6}$  mbar). The good thermal stability of  $\text{Cl}_8$ -PTCDI is evidenced by the high yield of the last purification step that afforded 350 mg of this organic semi-

[\*] M. Gsänger, A.-M. Krause, Prof. Dr. F. Würthner  
Universität Würzburg, Institut für Organische Chemie und  
Röntgen Research Center for Complex Material Systems  
Am Hubland, 97074 Würzburg (Germany)  
Fax: (+49) 931-318 4756  
E-mail: wuerthner@chemie.uni-wuerzburg.de

Dr. J. H. Oh, Prof. Dr. Z. Bao  
Stanford University, Department of Chemical Engineering  
381 North South Mall, Stanford, CA 94305 (USA)  
E-mail: zbao@stanford.edu

Dr. M. Könemann, Dr. H. W. Höffken  
BASF SE, 67056 Ludwigshafen (Germany)

[\*\*] This work was supported by the BMBF within Forum Organic Electronics, project 13N10205 PolytoS.

Supporting information for this article is available on the WWW under <http://dx.doi.org/10.1002/anie.200904215>.

conductor from 500 mg of pre-purified material. Moreover, block-shaped crystals could be obtained by this sublimation process, and were subjected to single-crystal X-ray analysis (Figure 2).<sup>[10]</sup>

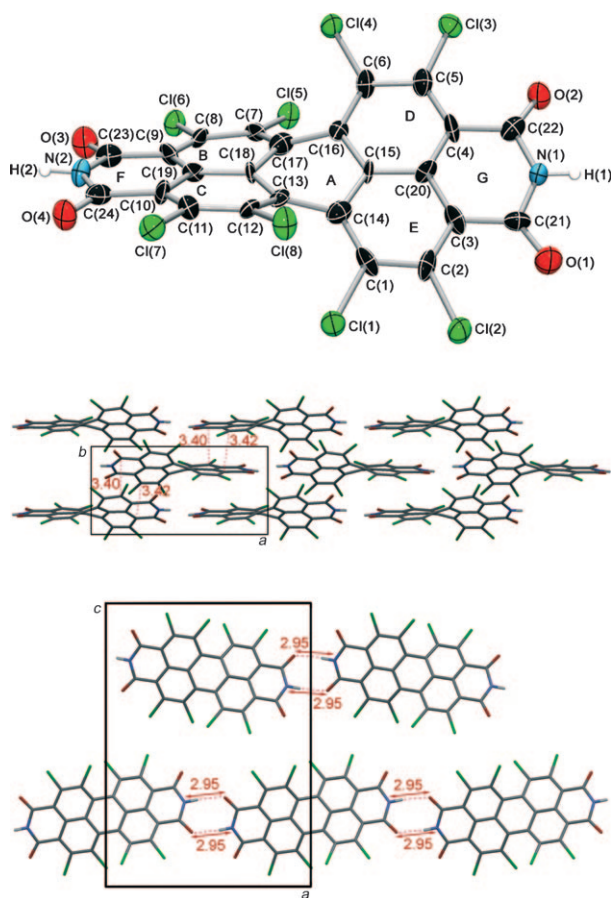


**Figure 2.** Molecular structure of Cl<sub>8</sub>-PTCDI in the crystal with numbering of atoms (top), packing arrangement by viewing onto the *a,b* plane (middle), and top view onto the *a,c* plane (bottom). Thermal ellipsoids are set at 50% probability.

The crystal structure of Cl<sub>8</sub>-PTCDI (Figure 2) shows a highly twisted perylene backbone with a dihedral angle of 37.2° between the planes of rings BCF and DEG marked in Figure 2. This structure is in good agreement with the results of other octachloro-substituted perylene diimides, for which the dihedral angle was determined to be 35.5° and the torsion angles 37° and 38°.<sup>[11]</sup> For Cl<sub>8</sub>-PTCDI, the torsion angles associated with the bay C atoms C(6)–C(16)–C(17)–C(7) and C(1)–C(14)–C(13)–C(12) are exactly the same, with a value of 35.8°. The closest intermolecular contact was found between the N(1) and O(3) atoms with a separation of 2.95 Å, which can be assigned to NH...O contacts between the imide hydrogen and the oxygen atoms of an imide group (Figure 2, bottom). The N...O distance of Cl<sub>8</sub>-PTCDI is in the range of the NH...O contacts in the DNA base pairs guanine/cytosine (2.84 Å) or adenine/thymine (2.82 Å),<sup>[12]</sup> and crystalline *N*-acetyl glycine (3.04 Å).<sup>[13]</sup> As in the case of tetrachlorinated perylene diimides<sup>[4]</sup> and other core-tetrasub-

stituted perylene diimides,<sup>[14]</sup> the twisted perylene core of Cl<sub>8</sub>-PTCDI induces conformational chirality, thus giving rise to the presence of *P* and *M* atropo-enantiomers in the solid state (Figure 2, middle). The longitudinal (along the N–N axis, pitch angle) and transverse (short molecular axis, roll angle) shifts of Cl<sub>8</sub>-PTCDI were calculated according to the method of Curtis et al.<sup>[15]</sup> Whilst a pitch angle of 63° could be determined, no shift was observed in transverse direction. Therefore the molecules in the crystal arrange in a slipped two-dimensional  $\pi$ -stacked layer with the shortest  $\pi$ – $\pi$  interactions of about 3.4 Å. This value is close to the interplane spacing of 3.37 Å for graphite,<sup>[16]</sup> and fits well to the range of 3.34–3.55 Å, which is known for core-unsubstituted perylene diimides.<sup>[17]</sup> This hydrogen-bond-enforced brickstone packing provides substantial  $\pi$ – $\pi$  overlap between each dye molecule and its four neighbors. Together with close chlorine–chlorine contacts (3.25–3.76 Å) in the third dimension and the quite high calculated density of this crystal structure (2.076 g cm<sup>−3</sup>), high electron mobilities for crystalline thin films of Cl<sub>8</sub>-PTCDI can be expected.

The electronic properties of the core-twisted Cl<sub>8</sub>-PTCDI were explored by UV/Vis absorption spectroscopy and cyclic voltammetry. In chloroform solution, Cl<sub>8</sub>-PTCDI shows a broad S<sub>0</sub>–S<sub>1</sub> transition band with an absorption maximum at 511 nm (28200 M<sup>−1</sup> cm<sup>−1</sup>) and vibronic progressions (see Figure S1 in the Supporting Information). A second maximum observed at 450 nm could be attributed to a higher-energy electronic transition.<sup>[9]</sup> Two reversible reduction waves were detected for Cl<sub>8</sub>-PTCDI by cyclic voltammetry in dichloromethane, with half-wave potentials of −0.57 V and −0.74 V versus ferrocene/ferrocenium (Fc/Fc<sup>+</sup>; Figure S2 in the Supporting Information). These waves correspond to the formation of radical anions and dianions of perylene diimide. No reversible oxidation could be observed for this electron-poor dye within the scanning range of the employed electrolyte (tetrabutyl ammonium hexafluorophosphate in dichloromethane). For comparison, perylene diimides without bay substituents are reduced at around −1.0 V and −1.2 V, and oxidized at about 1.2 V (vs. Fc/Fc<sup>+</sup>), while tetrachloro-substituted perylene diimides are reduced at around −0.87 V and −1.1 V (vs. Fc/Fc<sup>+</sup>) without showing any reversible oxidation.<sup>[4,17]</sup> Jones et al. reported the first reduction potential of dicyano-substituted perylene diimides to be around −0.45 V versus Fc/Fc<sup>+</sup>.<sup>[18]</sup> Accordingly, Cl<sub>8</sub>-PTCDI is amongst the most electron-deficient perylene diimide dyes reported so far, and thus one of the easiest to be reduced. Considering the energy level of Fc/Fc<sup>+</sup> at −4.8 eV with respect to the vacuum level,<sup>[19]</sup> the lowest unoccupied molecular orbital (LUMO) level of Cl<sub>8</sub>-PTCDI can be estimated as −4.8 eV − (−0.57 eV) = −4.23 eV, which, according to Jones et al., is clearly in the range of air-stable n-channel semiconductors.<sup>[18]</sup> The substantial decrease of the LUMO level of Cl<sub>8</sub>-PTCDI, despite its heavily twisted core, compared to core-unsubstituted (−3.7 eV) and tetrachloro-substituted perylene diimides (−3.8 eV) is indeed quite remarkable.<sup>[20]</sup>

Top-contact bottom-gate configuration OTFTs were fabricated with vapor-deposited Cl<sub>8</sub>-PTCDI films on a SiO<sub>2</sub> (300 nm) dielectric with an underlying n-doped silicon as the gate electrode. Subsequently, gold electrodes were

deposited through a shadow mask. The SiO<sub>2</sub> surface was modified with a crystalline self-assembled monolayer of *n*-octadecyl trimethoxysilane (OTS) by spin-coating as described previously.<sup>[8c]</sup> Various substrate temperatures (*T*<sub>D</sub>) were examined to optimize the electrical performance of Cl<sub>8</sub>-PTCDI films. The measured current–voltage characteristics of Cl<sub>8</sub>-PTCDI TFTs are summarized in Table 1. The field-effect mobilities ( $\mu$ ) were determined in the saturation regime from the slope of plots of (*I*<sub>DS</sub>)<sup>1/2</sup> versus *V*<sub>GS</sub> (Figure 3).

**Table 1:** TFT performance of Cl<sub>8</sub>-PTCDI on crystalline OTS-treated SiO<sub>2</sub>/Si substrates.<sup>[a]</sup>

<i>T</i> <sub>D</sub> [°C]	In N <sub>2</sub> atmosphere			After exposure to air		
	$\mu$ [cm <sup>2</sup> V <sup>−1</sup> s <sup>−1</sup> ]	<i>I</i> <sub>on</sub> / <i>I</i> <sub>off</sub>	<i>V</i> <sub>t</sub> [V]	$\mu$ [cm <sup>2</sup> V <sup>−1</sup> s <sup>−1</sup> ]	<i>I</i> <sub>on</sub> / <i>I</i> <sub>off</sub>	<i>V</i> <sub>t</sub> [V]
25	3.1 × 10 <sup>−3</sup>	5.0 × 10 <sup>4</sup>	41	7.5 × 10 <sup>−4</sup>	5.3 × 10 <sup>4</sup>	39
90	0.87	2.3 × 10 <sup>7</sup>	45	0.56	8.4 × 10 <sup>7</sup>	47
125	0.91	2.1 × 10 <sup>7</sup>	28	0.82	1.5 × 10 <sup>8</sup>	28
150	0.90	5.1 × 10 <sup>6</sup>	36	0.75	8.1 × 10 <sup>6</sup>	37

[a] *I*–*V* measurements were carried out inside an N<sub>2</sub>-filled glove box (O<sub>2</sub> level < 1 ppm) as well as under an ambient laboratory environment at about 1 h after exposure to air. The observed maximum mobility and the corresponding on/off ratio are given.

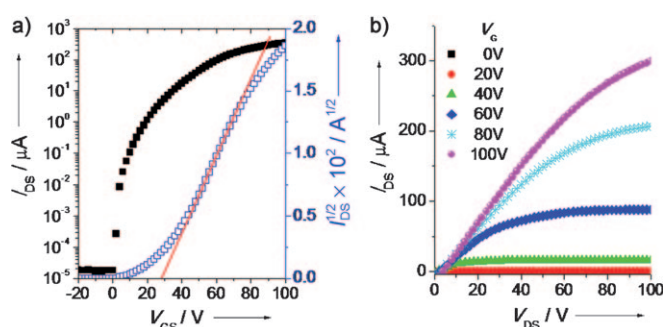


**Figure 3.** *I*–*V* characteristics of Cl<sub>8</sub>-PTCDI TFT prepared on OTS-treated SiO<sub>2</sub>/Si at *T*<sub>D</sub> = 125 °C. a) Plot of *I*<sub>DS</sub> vs. *V*<sub>GS</sub> for *V*<sub>DS</sub> = 100 V. b) Plot of *I*<sub>DS</sub> vs. *V*<sub>DS</sub>. The measurement was carried out under nitrogen atmosphere.

In a nitrogen atmosphere, the mobility of Cl<sub>8</sub>-PTCDI on the OTS-treated SiO<sub>2</sub>/Si increased significantly from 3.1 × 10<sup>−3</sup> to 0.91 cm<sup>2</sup>V<sup>−1</sup>s<sup>−1</sup> by increasing the *T*<sub>D</sub> value from 25 to 125 °C, which corresponds to the optimized *T*<sub>D</sub> value generally observed for PTCDI-based semiconductors.<sup>[6,21,22]</sup> At *T*<sub>D</sub> = 125 °C, Cl<sub>8</sub>-PTCDI TFT devices showed an on-to-off current ratio (*I*<sub>on</sub>/*I*<sub>off</sub>) as high as 10<sup>7</sup> and a threshold voltage (*V*<sub>t</sub>) of 28 V (Figure 3). Owing to the energetically low-lying LUMO, the Cl<sub>8</sub>-PTCDI TFTs exhibited air-stable operation with a mobility as high as 0.82 cm<sup>2</sup>V<sup>−1</sup>s<sup>−1</sup> with *I*<sub>on</sub>/*I*<sub>off</sub> of 10<sup>8</sup>; the *V*<sub>t</sub> value is hardly shifted compared to that measured in a nitrogen atmosphere. The mobility is 7.5 times higher than that of Cl<sub>4</sub>-PTCDI (0.11 cm<sup>2</sup>V<sup>−1</sup>s<sup>−1</sup>), which contains four chlorine atoms in the core,<sup>[6a]</sup> and compares well to the best performance achieved for crystal-engineered p-channel pentacene derivatives.<sup>[3]</sup> It is striking that such high mobilities are

obtained from the nonplanar, contorted  $\pi$ -conjugated molecules.

A structural analogue of Cl<sub>8</sub>-PTCDI, 1,2,5,6,7,8,11,12-octachloroperylene-3,4:9,10-tetracarboxylic dianhydride (Cl<sub>8</sub>-PTCDA), where the NH group is replaced by an O atom, showed much lower mobilities (ca. 10<sup>−5</sup> cm<sup>2</sup>V<sup>−1</sup>s<sup>−1</sup>). We assume that the efficient charge transport in Cl<sub>8</sub>-PTCDI TFTs originates from the hydrogen-bond-directed dense brickstone packing of Cl<sub>8</sub>-PTCDI, where substantial  $\pi$ – $\pi$  orbital overlaps with the close  $\pi$ -plane distance of approximately 3.4 Å are realized in two dimensions. The close chlorine–chlorine contacts in the third dimension might also provide a percolation pathway for electrons. In addition to the high electron mobility, the exceptionally high *I*<sub>on</sub>/*I*<sub>off</sub> ratio and the minimal shift of *V*<sub>t</sub> in air make this material very promising for diverse applications that require high-performance air-stable n-channel organic semiconductors. Remarkably, these excellent charge carrier mobility values and on/off ratios are almost unchanged even after exposing the devices to air for about 20 months ( $\mu \approx 0.60$  cm<sup>2</sup>V<sup>−1</sup>s<sup>−1</sup>, *I*<sub>on</sub>/*I*<sub>off</sub>  $\approx 10^7$ ). The air-stability of these n-channel transistors is probably due to the energetically low-lying LUMO and the high packing density of Cl<sub>8</sub>-PTCDI.

The microstructure of the vapor-deposited Cl<sub>8</sub>-PTCDI thin films was analyzed by atomic force microscopy (AFM) and out-of-plane X-ray diffraction (XRD). Unlike most other PTCDI derivatives, which tend to form needle-like crystals, Cl<sub>8</sub>-PTCDI formed large two-dimensional grains. As generally observed for organic semiconductors, AFM images revealed that the grain size becomes larger with increasing *T*<sub>D</sub>, which leads to the increased mobilities (Figure S3 in the Supporting Information). As the data in Table 1 show, the field-effect mobility at *T*<sub>D</sub> = 150 °C decreased compared to that at 125 °C, which is presumably due to the increased empty space between the grains and crack formation in the films upon cooling.<sup>[6b,21,23]</sup> The morphology of Cl<sub>8</sub>-PTCDI films on bare SiO<sub>2</sub>/Si was found to have smaller grains compared to that on OTS-treated SiO<sub>2</sub>/Si (Figure S4 in the Supporting Information). As a result, TFT devices prepared on bare SiO<sub>2</sub>/Si substrates showed mobilities three orders of magnitude lower than OTS-treated SiO<sub>2</sub>/Si substrates (see Table S1 in Supporting Information). The XRD measurements of 45 nm thick films of Cl<sub>8</sub>-PTCDI deposited onto OTS-treated SiO<sub>2</sub>/Si substrates exhibited the primary peak at 2 $\theta$  = 8.58° and higher peak intensities at higher *T*<sub>D</sub> values. This value corresponds to a *d* spacing of 10.30 Å (Figure S5 in the Supporting Information) and is close to the geometry-optimized, computed molecular length along the long axis of the molecule (13.36 Å). This result indicates that the Cl<sub>8</sub>-PTCDI molecules adopt an edge-on conformation in thin films. In contrast, no discernible XRD peak was observed for Cl<sub>8</sub>-PTCDI thin films evaporated onto bare SiO<sub>2</sub>/Si substrates across all the *T*<sub>D</sub> values, thus revealing the amorphous features of the thin films. The lower charge-carrier mobility of the Cl<sub>8</sub>-PTCDI films on bare SiO<sub>2</sub>/Si could thus be attributed to the poorer intermolecular interactions within the amorphous films, and morphological issues, as well as to the increased charge trapping by hydroxyl groups at the dielectric/semiconductor interface.<sup>[23–25]</sup> It is noteworthy that peaks due to other phases



and/or orientations (P2) exist in addition to the primary phase (P1) in the Cl<sub>8</sub>-PTCDI film deposited on OTS-treated substrate at a  $T_D = 125^\circ\text{C}$ . These peaks may originate from the presence of different polymorphs in the solid state, in conjunction with *P* and *M* atropo-enantiomers, because of the core-twisted character of Cl<sub>8</sub>-PTCDI. This characteristic is similar to that observed for tetrafluoro-PTCDI.<sup>[22]</sup>

In summary, we have demonstrated a molecular and crystal engineering approach towards high-performance n-channel OTFTs based on a perylene diimide semiconductor. An increase in the number of chlorine substituents at the perylene core from four to eight ("molecular engineering") affords a substantial lowering of the LUMO level, whilst the combination of hydrogen bonding and contortion of the  $\pi$  core directs two-dimensional  $\pi$ - $\pi$ -stacked percolation paths for electron transport ("crystal engineering"). As a consequence of this molecular design, Cl<sub>8</sub>-PTCDI-based TFTs can operate in air with excellent electron mobility and high  $I_{\text{on}}/I_{\text{off}}$  ratio.

Received: July 29, 2009

Published online: October 30, 2009

**Keywords:** crystal engineering · dyes/pigments · hydrogen bonding · organic semiconductors · thin film transistors

- [1] a) J. A. Anthony, *Angew. Chem.* **2008**, *120*, 460–492; *Angew. Chem. Int. Ed.* **2008**, *47*, 452–483; b) H. E. Katz, Z. Bao, S. L. Gilat, *Acc. Chem. Res.* **2001**, *34*, 359–369; c) F. Würthner, R. Schmidt, *ChemPhysChem* **2006**, *7*, 793–797.
- [2] For general reviews, see: a) G. R. Desiraju, A. Gavezzotti, *Acta Crystallogr. Sect. B* **1989**, *45*, 473–482; b) G. R. Desiraju, *Angew. Chem.* **1995**, *107*, 2541–2558; *Angew. Chem. Int. Ed. Engl.* **1995**, *34*, 2311–2327; c) G. R. Desiraju, *Acc. Chem. Res.* **2002**, *35*, 565–573; d) P. Erk, H. Hengelsberg, M. F. Haddow, R. van Gelder, *CrystEngComm* **2004**, *6*, 474–483.
- [3] a) C. D. Sheraw, T. N. Jackson, D. L. Eaton, J. E. Anthony, *Adv. Mater.* **2003**, *15*, 2009–2011; b) M. M. Payne, S. R. Parkin, J. E. Anthony, C. Kuo, T. N. Jackson, *J. Am. Chem. Soc.* **2005**, *127*, 4986–4987; c) H. Moon, R. Zeis, E. J. Borkent, C. Besnard, A. J. Lovinger, T. Siegrist, C. Kloc, Z. Bao, *J. Am. Chem. Soc.* **2004**, *126*, 15322–15323; d) for another interesting strategy to shift herringbone packing to brickstone stacking, see: A. Facchetti, M.-H. Yoon, C. L. Stern, H. E. Katz, T. J. Marks, *Angew. Chem.* **2003**, *115*, 4030–4033; *Angew. Chem. Int. Ed.* **2003**, *42*, 3900–3903.
- [4] Z. Chen, M. G. Debije, T. Debaerdemaeker, P. Osswald, F. Würthner, *ChemPhysChem* **2004**, *5*, 137–140.
- [5] S. X. Xiao, M. Myers, Q. Miao, S. Sanaur, K. L. Pang, M. L. Steigerwald, C. Nuckolls, *Angew. Chem.* **2005**, *117*, 7556–7560; *Angew. Chem. Int. Ed.* **2005**, *44*, 7390–7394.
- [6] a) M. M. Ling, P. Erk, M. Gomez, M. Könnemann, J. Locklin, Z. Bao, *Adv. Mater.* **2007**, *19*, 1123–1127; b) R. Schmidt, J. H. Oh, Y.-S. Sun, M. Deppisch, A.-M. Krause, K. Radacki, H. Braunschweig, M. Könnemann, P. Erk, Z. Bao, F. Würthner, *J. Am. Chem. Soc.* **2009**, *131*, 6215–6228.
- [7] T. Kaiser, H. Wang, V. Stepanenko, F. Würthner, *Angew. Chem.* **2007**, *119*, 5637–5640; *Angew. Chem. Int. Ed.* **2007**, *46*, 5541–5544.
- [8] For other recent n-type OTFTs with outstanding electron mobility, see: a) A. S. Molinari, H. Alves, Z. Chen, A. Facchetti, A. F. Morpurgo, *J. Am. Chem. Soc.* **2009**, *131*, 2462–2463; b) H. Yan, Z. Chen, Y. Zheng, C. Newman, J. R. Quinn, F. Dötz, M. Kastler, A. Facchetti, *Nature* **2009**, *457*, 679–686; c) Y. Ito, A. A. Virkar, S. Mannsfeld, J. H. Oh, M. Toney, J. Locklin, Z. Bao, *J. Am. Chem. Soc.* **2009**, *131*, 9396–9404.
- [9] For an early report of octachlorinated perylene diimides and perylene dianhydrides, see: M. Sadrai, L. Hadel, R. R. Sauers, S. Husain, K. Krogh-Jespersen, J. D. Westbrook, G. R. Bird, *J. Phys. Chem.* **1992**, *96*, 7988–7996.
- [10] Characterization data for Cl<sub>8</sub>-PTCDI: M.p. > 350 °C; <sup>1</sup>H NMR (600 MHz, [D<sub>6</sub>]DMSO, 50 °C):  $\delta = 12.19$  ppm (s, 2H; NH); HRMS (ESI, negative mode, acetonitrile/CHCl<sub>3</sub> 1:1):  $m/z$ : 660.7450 [ $M^-$ –H] (calcd for C<sub>24</sub>HCl<sub>8</sub>N<sub>2</sub>O<sub>4</sub> 660.7450); UV/Vis (CHCl<sub>3</sub>):  $\lambda_{\text{max}}$  ( $\epsilon$ ) = 511 (28200), 480 (22500), 449 nm (21400 m<sup>−1</sup> cm<sup>−1</sup>); elemental analysis calcd (%) for C<sub>24</sub>H<sub>2</sub>Cl<sub>8</sub>N<sub>2</sub>O<sub>4</sub>: C 43.29, H 0.30, N 4.21; found C 43.28, H 0.63, N 4.17. Crystal data for Cl<sub>8</sub>-PTCDI: C<sub>24</sub>H<sub>2</sub>Cl<sub>8</sub>N<sub>2</sub>O<sub>4</sub>,  $M_r = 665.91$ , pale yellow block, 0.4 × 0.2 × 0.1 mm<sup>3</sup>, orthorhombic space group Pbcn,  $a = 14.455(2)$ ,  $b = 7.3585(13)$ ,  $c = 20.033(3)$  Å,  $\alpha = \beta = \gamma = 90^\circ$ ,  $V = 2130.9(6)$  Å<sup>3</sup>,  $Z = 4$ ,  $\rho_{\text{calcd}} = 2.076$  g cm<sup>−3</sup>,  $\mu = 10.069$  mm<sup>−1</sup>,  $F(000) = 1312$ ,  $T = 100(2)$  K,  $R_1 = 0.0783$ ,  $wR^2 = 0.1988$ , 1232 independent reflections [ $2\theta \leq 58.10^\circ$ ] and 173 parameters. CCDC 738649 contains the supplementary crystallographic data for this paper. These data can be obtained free of charge from The Cambridge Crystallographic Data Centre via [www.ccdc.cam.ac.uk/data\\_request/cif](http://www.ccdc.cam.ac.uk/data_request/cif).
- [11] M. Sadrai, G. R. Bird, J. A. Potenza, H. J. Schugar, *Acta Crystallogr. Sect. C* **1990**, *46*, 637–640.
- [12] D. S. Johnson, D. L. Boger in *Comprehensive Supramolecular Chemistry*, Vol. 4 (Eds.: J. L. Atwood, J. E. D. Davies, D. D. MacNicol, F. Vögtle, Y. Murakami), Pergamon, Oxford, **1996**, p. 76.
- [13] Z. Berkovitch-Yellin, S. Ariel, L. Leiserowitz, *J. Am. Chem. Soc.* **1983**, *105*, 765–767.
- [14] P. Osswald, F. Würthner, *J. Am. Chem. Soc.* **2007**, *129*, 14319–14326.
- [15] M. D. Curtis, J. Cao, J. W. Kampf, *J. Am. Chem. Soc.* **2004**, *126*, 4318–4328.
- [16] S. R. Forrest, M. L. Kaplan, P. H. Schmidt, *J. Appl. Phys.* **1984**, *55*, 1492–1507.
- [17] G. Klebe, F. Graser, E. Hädicke, J. Berndt, *Acta Crystallogr. Sect. B* **1989**, *45*, 69–77.
- [18] B. A. Jones, A. Facchetti, M. R. Wasielewski, T. J. Marks, *J. Am. Chem. Soc.* **2007**, *129*, 15259–15278.
- [19] I. Seguy, P. Jolinat, P. Destruel, R. Mamy, H. Allouchi, C. Courseille, M. Cotrait, H. Bock, *ChemPhysChem* **2001**, *2*, 448–452.
- [20] For a comparison of reduction potentials of core-substituted perylene diimides, see: F. Würthner, *Chem. Commun.* **2004**, 1564–1579.
- [21] J. H. Oh, S. Liu, Z. Bao, R. Schmidt, F. Würthner, *Appl. Phys. Lett.* **2007**, *91*, 212107.
- [22] R. Schmidt, M. M. Ling, J. H. Oh, M. Winkler, M. Könnemann, Z. Bao, F. Würthner, *Adv. Mater.* **2007**, *19*, 3692–3695.
- [23] R. J. Chesterfield, J. C. McKeen, C. R. Newman, P. C. Ewbank, D. A. da Silva, J. L. Bredas, L. L. Miller, K. R. Mann, C. D. Frisbie, *J. Phys. Chem. B* **2004**, *108*, 19281–19292.
- [24] B. Yoo, T. Jung, D. Basu, A. Dodabalapur, B. A. Jones, A. Facchetti, M. R. Wasielewski, T. J. Marks, *Appl. Phys. Lett.* **2006**, *88*, 082104.
- [25] L. L. Chua, J. Zaumseil, J. F. Chang, E. C. W. Ou, P. K. H. Ho, H. Sirringhaus, R. H. Friend, *Nature* **2005**, *434*, 194–199.